

The family of curves shown in Fig. 4 were drawn in the same manner as those of Fig. 3. A curve whose shape is the same as those of Fig. 3 was

drawn through the sodium yield points. Curves for other values of ΔZ were then drawn such that K corresponds to a value of 1.6.

*Research sponsored in part by the U. S. Atomic Energy Commission under contract with Union Carbide Corporation.

†Present address: Knoxville College, Knoxville, Tennessee 37916.

‡Present address: U. S. Atomic Energy Commission, New Brunswick, New Jersey.

§On training act from the National Bureau of Standards, Washington, D. C. 20234, 1967-1968.

¹Both photodisintegration and electrodisintegration reactions occur; by use of the virtual-photon concept, originally proposed by C. F. Weizacker, *Z. Physik* **88**, 612 (1934) and E. J. Williams, *Phys. Rev.* **45**, 729 (1934), electrodisintegration at high energy may be regarded as a photonuclear reaction. In the work reported in this paper no distinction is made between real and virtual photons.

²G. B. Collins, B. Waldman, and E. Guth, *Phys. Rev.* **56**, 876 (1939).

³W. Paul, *Naturium* **36**, 31 (1949).

⁴L. S. Skaggs, J. S. Laughlin, A. O. Hanson, and J. J. Orlin, *Phys. Rev.* **73**, 420 (1948).

⁵K. L. Brown and R. Wilson, *Phys. Rev.* **93**, 443 (1954).

⁶R. L. Hines, *Phys. Rev.* **105**, 1534 (1957).

⁷W. C. Barber, *Phys. Rev.* **111**, 1642 (1958).

⁸W. C. Barber and T. Wiedling, *Nucl. Phys.* **18**, 575 (1960).

⁹C. B. Fulmer, I. R. Williams, T. H. Handley, G. F. Dell, and L. N. Blumberg, *Phys. Rev. Letters* **19**, 522

(1967).

¹⁰H. W. Bertini, *Phys. Rev.* **131**, 1801 (1963); **138** AB2 (E) (1965); Oak Ridge National Laboratory Report No. ORNL-TM-1225, 1965 (unpublished).

¹¹Y. S. Tsai and V. Whitis, *Phys. Rev.* **149**, 1248 (1966).

¹²E. L. Callis, Oak Ridge National Laboratory Report No. ORNL-TM-2309, 1969 (unpublished).

¹³J. M. Miller and J. Hudis, *Ann. Rev. Nucl. Sci.* **9**, 159 (1959).

¹⁴R. W. Spence and G. P. Ford, *Ann. Rev. Nucl. Sci.* **2**, 411 (1953).

¹⁵W. D. Myers and W. J. Swiatecki, *Nucl. Phys.* **81**, 1 (1966).

¹⁶C. B. Fulmer, I. R. Williams, K. S. Toth, and G. F. Dell, *Phys. Rev.* **188**, 1752 (1969).

¹⁷B. Rossi, *High Energy Particles* (Prentice-Hall, Inc., Englewood Cliffs, New Jersey, 1952).

¹⁸C. E. Roos and V. Z. Peterson, *Phys. Rev.* **124**, 1610 (1961).

¹⁹I. Halpern, R. J. Debs, J. T. Eisinger, A. W. Fairhall, and H. G. Richter, *Phys. Rev.* **97**, 1327 (1955).

²⁰I. Dostrovsky, Z. Fraenkel, and G. Friedlander, *Phys. Rev.* **116**, 683 (1959).

²¹H. W. Schmitt, private communication.

²²J. Wing and P. Fong, *Phys. Rev.* **136**, B923 (1964).

²³S. Katcoff, H. R. Fickel, and A. Wyttenbach, *Phys. Rev.* **166**, 1147 (1968).

²⁴R. H. Lindsay, *Phys. Rev.* **147**, 792 (1966).

²⁵J. R. Nix and E. Sassi, *Nucl. Phys.* **81**, 61 (1966).

Excitation Functions for the Reactions $^{34}\text{S}(p, n)^{34}\text{Cl}$ and $^{31}\text{P}(\alpha, n)^{34}\text{Cl}^\dagger$

C. J. Umbarger,* K. W. Kemper, J. W. Nelson, and H. S. Plendl

Department of Physics, The Florida State University, Tallahassee, Florida 32306

(Received 25 May 1970)

Excitation curves for $^{34}\text{S}(p, n)^{34}\text{Cl}$ and $^{31}\text{P}(\alpha, n)^{34}\text{Cl}$ were measured from the observed thresholds at 6438 ± 10 and 6360 ± 10 keV, respectively, to 1.6 MeV above threshold by detecting the residual radioactivity. Two prominent resonant structures were found in both reactions at the same excitation energies, 12.9 and 13.9 MeV, in the compound nucleus ^{35}Cl . Excitation curves for $^{31}\text{P}(\alpha, n)$ were also measured in the region of these resonances, but no similar prominent resonances were found. Arguments are presented that indicate a $T = \frac{3}{2}$ assignment for these resonances. Absolute values of the total cross section were determined for the above (p, n) and (α, n) reactions and also for $^{34}\text{S}(p, n)^{34}\text{Cl}^m$ and $^{31}\text{P}(\alpha, n)^{34}\text{Cl}^m$.

I. INTRODUCTION

Proton scattering as well as proton-induced reactions have become a well-established tool for the observation of isobaric analog states. These

states are generally studied by analyzing the compound-nucleus resonances which appear in excitation curves. The analog states observed in the proton-plus-target system have isospin $T_0 + \frac{1}{2} \equiv T_+$, where T_0 is the target isospin. These states are

analogous to lower-lying parent states in the adjacent neutron-plus-target system, which have the same (T, J^π) assignments but a different T_z value. Together with the parent states, the analog states constitute part of an isospin multiplet. In addition to $T_>$ states, protons can also excite levels having $T_0 - \frac{1}{2} \equiv T_<$. The $T_<$ states have a much higher density than the $T_>$ states and form a more or less continuous background (especially at high excitation energies) to the superimposed $T_>$ levels.

The analog states observed in the proton-plus-target system can also be seen as compound-nucleus resonances in α -particle scattering and in α -particle-induced reactions on the appropriate target ($Z_\alpha = Z_p - 1$, $A_\alpha = A_p - 3$). The ease with which $T_>$ analog states can be observed in α -particle-induced reactions depends on the amount of isospin mixing in the compound nucleus and, to a lesser extent, in the target and α -particle itself. No isospin mixing is necessary for $T_<$ states to be excited by either protons or α particles on their respective targets.

The present work provides information on the structure of the compound nucleus ^{35}Cl above 12.5-MeV excitation energy. Excitation functions for both the $^{34}\text{S}(p, n)$ and the $^{31}\text{P}(\alpha, n)$ reaction were measured from 6.3- to 7.9-MeV incident proton and α -particle energy, respectively. This range corresponds to excitation energies from 12.5 to 14.0 MeV in the compound nucleus ^{35}Cl and to excitation energies up to 1.6 MeV in the product nucleus ^{34}Cl . The excitation functions revealed the existence of well-isolated resonances. Two of the more prominent resonances found in the (p, n) excitation curve were found to occur at the same excitation energy in ^{35}Cl as two prominent resonances in the (α, n) curve. These two resonances are attributed to isobaric analog states in ^{35}Cl with parent states in ^{35}S . To help assign isospin values to these resonances, $^{31}\text{P}(\alpha, \alpha_0)^{31}\text{P}$ excitation functions were measured over the resonance regions at 15 angles with respect to the incident beam.

Previously published work on the $^{31}\text{P}(\alpha, n)$ ¹ and $^{34}\text{S}(p, n)$ ² reactions is limited to the measurement of the relative-yield excitation curves at and immediately above the ground-state threshold. In the present work, the thresholds of these reactions have been redetermined and used to calculate a consistent value for the mass of the product nucleus ^{34}Cl .

II. EXPERIMENTAL PROCEDURE

Targets for the $^{34}\text{S}(p, n)$ and $^{31}\text{P}(\alpha, n)$ excitation functions were prepared by evaporating enriched CdS onto 0.12-mm gold plate and natural Ca_3P_2 onto 0.075-mm tantalum plate, respectively. The

CdS material (enriched in ^{34}S to 14.9%) was obtained from the Oak Ridge National Laboratory (ORNL). The target thickness at the bombarding energy was 10 keV for the CdS target and 80 keV for the Ca_3P_2 target. The targets used for the absolute cross-section measurements were AgS for the (p, n) and natural Ca_3P_2 for the (α, n) work. The AgS target was prepared by heating sulfur (enriched in ^{34}S to 67% and also obtained from ORNL) in the presence of 0.025-mm Ag foil. The Ca_3P_2 target was evaporated onto 0.025-mm-thick Al foil. The thickness of the targets was determined by weighing.

The proton and α -particle beams were obtained from the Florida State University Tandem Van de Graaff accelerator. The beam-energy analyzing system has been calibrated^{3,4} by measurement of a series of (p, n) and (α, n) thresholds. The calibration was frequently rechecked throughout this work with the $^{27}\text{Al}(p, n)^{27}\text{Si}$ threshold. A threshold value of 5800 ± 3 keV was used, which is the mean of the results reported by Bonner *et al.*⁵ and Freeman *et al.*²

The (p, n) and (α, n) excitation curves shown in Figs. 1 to 4 were determined by measuring the residual activity of the product nucleus ^{34}Cl as a function of bombarding energy with an activation-analysis technique. This "beam-off" experiment resulted in a high yield-to-background ratio, and contributions to the yield from target backing, target contaminants, and competing reactions were almost completely eliminated.

The superallowed, $0^+(\beta^+)0^+$, excitation curve was determined by direct detection of the posi-

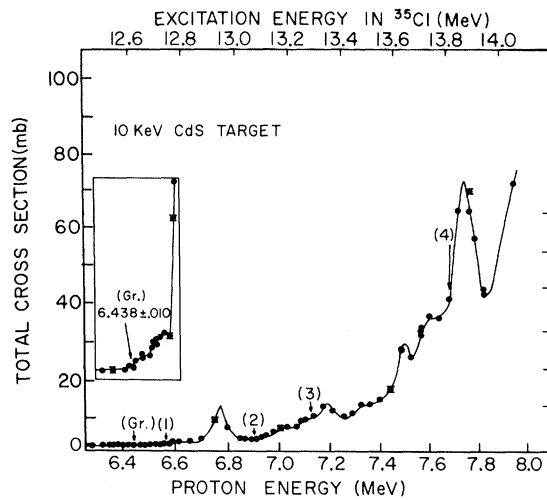


FIG. 1. Thin-target excitation curve for $^{34}\text{S}(p, n)^{34}\text{Cl}$ obtained by measuring the positrons from the superallowed β decay of ^{34}Cl . Location of the thresholds expected for known states of ^{34}Cl (labeled by the numbers in parentheses) are shown for reference. The ground-state threshold is shown in more detail in the inset.

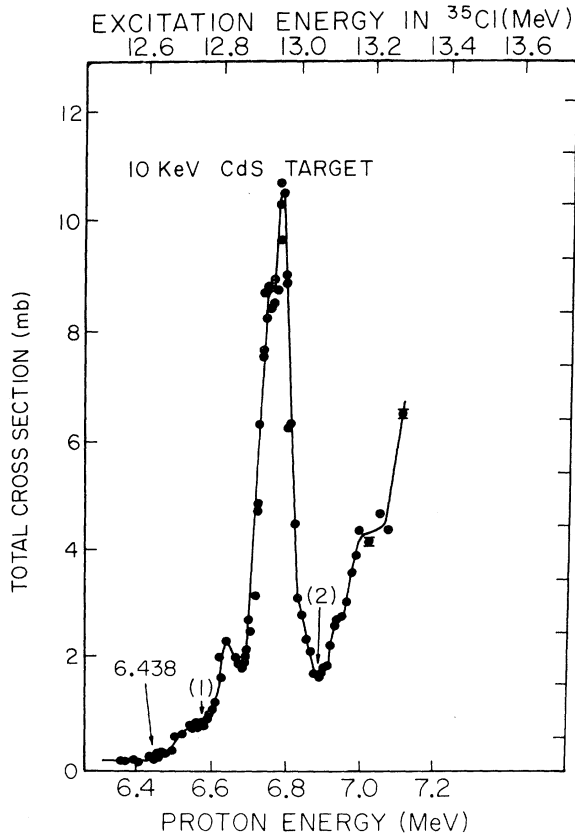


FIG. 2. Excitation curve for $^{34}\text{S}(p,n)^{34}\text{Cl}$ showing in detail the resonant structure in the region near 12.9-MeV excitation energy in ^{35}Cl .

trons from the ^{34}Cl ground-state decay in a 5.0×5.0 -cm plastic scintillator (NE102). The bombardment times, waiting periods, and counting times were automatically controlled by a "leaky" integrator circuit.⁶ The amplified scintillator signals corresponding to $E_{\beta^+} \geq 1.3$ MeV were fed into a multichannel analyzer operating in a multi-scaler mode. In this mode the target activity was measured as a function of time. The total counting time was 6.4 sec, or about four half-lives. A relative measure of the yield for each point on the excitation curve was obtained by subtracting the sum of the counts in the last 1.5 sec of the counting period from the sum of the counts in the first 1.5 sec.

The relative total cross section was normalized to an absolute scale by measuring the absolute total cross section at several points on the curve. This was done by a direct measurement of the high-energy portion of the emitted β^+ spectrum. This portion was compared with the theoretical spectrum for superallowed β^+ decay. The area of the undetected part of the spectrum was then added to the observed portion to obtain the total number

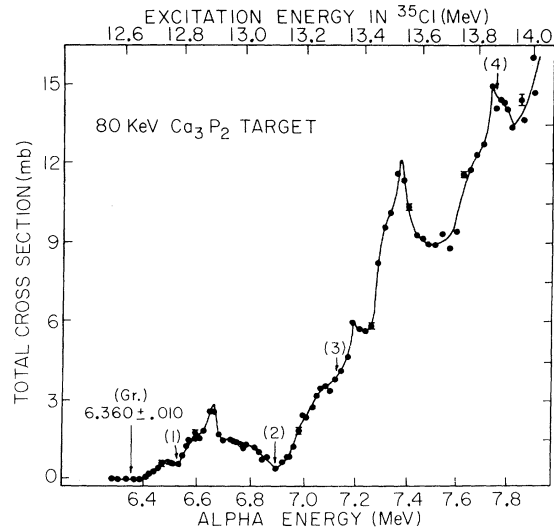


FIG. 3. Excitation curve for $^{31}\text{P}(\alpha,n)^{34}\text{Cl}$ obtained by measuring positrons of the superallowed β decay of ^{34}Cl . Resonant structure is evident in the region of excitation near 12.9 MeV in ^{35}Cl , just as it is in the $^{34}\text{S}(p,n)^{34}\text{Cl}$ excitation curve of Fig. 1. Numbers in parenthesis indicate the expected locations of thresholds for known levels of ^{34}Cl .

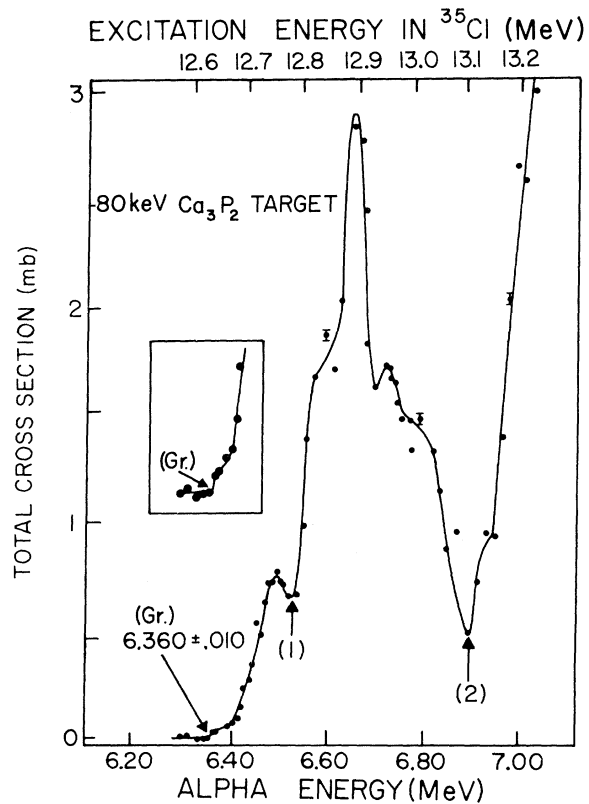


FIG. 4. Excitation curve for $^{31}\text{P}(\alpha,n)^{34}\text{Cl}$ showing in detail the resonant structure near 12.9-MeV excitation in ^{35}Cl , which corresponds to the resonant structure in the $^{34}\text{S}(p,n)^{34}\text{Cl}$ excitation curve of Fig. 2.

of positrons emitted. The "leaky" integrator was used to control the bombarding and counting cycles. The positrons were collimated and detected in a 7.5×10 -cm plastic scintillator (NE102).

The allowed excitation function was determined by measurement of the 2.127-MeV γ ray in ^{34}S which follows the allowed positron decay of the 3^+ isomeric state in ^{34}Cl . The "leaky" integrator was used to control the bombardment and counting cycle, and the γ rays were counted in a 15-cm³ Ge(Li) detector. After correction for decay branching, the absolute total cross section for formation of the 3^+ level was determined at several beam energies.

Errors in the absolute values of the cross sections were estimated to be $\pm 10\%$ for the excitation curves obtained by measurement of the superallowed decay and $\pm 14\%$ for the allowed decay. The major contribution to these errors was the uncertainty in target density, with an additional error due to uncertainties in the determination of the Ge(Li) detector efficiency for the allowed decay.

III. EXPERIMENTAL RESULTS AND DISCUSSION

The ground-state threshold for the $^{34}\text{S}(p, n)^{34}\text{Cl}$ reaction was determined to be 6438 ± 10 keV. The inset in Fig. 1 shows, in detail, the superallowed excitation function near threshold. The location of the threshold for the first excited state in ^{34}Cl is indicated in Figs. 1 and 2 by (1). An increase in yield at this energy could indicate that the first excited state has been reached. However, due to the much longer half-life of this state compared with the ground state (32 min versus 1.6 sec), any yield from the 3^+ state would be nearly equal in both the yield and background β spectra and hence cancel. Accordingly, the increase in yield labeled (1) in Figs. 1 and 2 is attributed to resonance effects.

As can be seen from Figs. 1 and 2, the entire excitation function from the ground-state threshold to above the location for the fourth excited state contains evidence of resonance contributions. The positions marked by numbers in parentheses indicate the locations of thresholds for known levels of ^{34}Cl taken from the compilation of Endt and Van der Leun.⁷ The peak near 6.78 MeV in Fig. 1 was drawn using the data from Fig. 2 as a guide. That figure shows the excitation function over this limited region in detail.

The ground-state threshold for the $^{31}\text{P}(\alpha, n)^{34}\text{Cl}$ reaction was determined to be 6360 ± 10 keV. Figure 3 shows the excitation function to above the position for the fourth excited state, and Fig. 4 shows the region at and above the ground-state

threshold in detail. Expected locations for the excited-state thresholds are indicated. The energy scales on the top of Figs. 1 to 4 give the excitation energies in the compound nucleus ^{35}Cl to facilitate a direct comparison of the (p, n) resonances with those found in the (α, n) excitation curve.

The ground-state-threshold results obtained from this work, and previously published values are listed in Table I, together with the corresponding Q values and ^{34}Cl mass-excess values. The present measurements agree with the earlier work within experimental errors. The mass-excess values for ^{34}Cl , determined from the present (p, n) and (α, n) ground-state-threshold results and known mass-excess values for the target nuclei,⁷ also agree with one another within experimental errors. The 10-keV error assignment to the thresholds is composed of the error in the absolute energy calibration (± 6 keV) and the uncertainty in the threshold determination (± 8 keV).

The $^{34}\text{S}(p, n)^{34}\text{Cl}^m$ and $^{31}\text{P}(\alpha, n)^{34}\text{Cl}^m$ excitation functions measured over a limited energy range are shown in Figs. 5 and 6, respectively. The superallowed excitation functions measured over the same energy region (see Figs. 2 and 4) are also shown for comparison. The excitation functions have been normalized to the absolute total cross-section scales shown at the left of the figures. Figures 5 and 6 reveal that the compound-nucleus resonances found in the superallowed curves do not correspond to the resonances in the allowed curves. Thus the resonance phenomenon is associated with compound-nucleus neutron decay to the $T=1$ product nucleus ground state and not with neutron decay to the $T=0$ isomeric state.

In the Endt and Van der Leun compilation,⁷ 14 $^{31}\text{P}(\alpha, p_0)^{34}\text{S}$ resonances are shown between 9.13 and 9.93 MeV in ^{35}Cl . In addition, 48 $^{34}\text{S}(p, \gamma)^{35}\text{Cl}$ resonances are shown between 7.06 and 8.96 MeV, so that the mean level spacing is less than 40 keV. No information is available for ^{35}Cl excitation energies above 9.93 MeV, but the level density should be just as high or higher.

In addition to many small resonances, two prom-

TABLE I. Comparison of ground-state threshold results. (The errors are threshold experimental errors only.)

Reaction	Ground-state threshold (keV)	Corresponding Q value (keV)	^{34}Cl Mass excess (keV)
$^{34}\text{S}(p, n)^{34}\text{Cl}$	6438 ± 10^a	-6254 ± 10^a	$-24\,462 \pm 10$
	6451 ± 5^b	-6267 ± 5^b	$-24\,449 \pm 5$
$^{31}\text{P}(\alpha, n)^{34}\text{Cl}$	6360 ± 10^a	-5633 ± 10^a	$-24\,451 \pm 10$
	6440 ± 200^c	-5700 ± 200^c	$-24\,384 \pm 200$

^aPresent work.

^bSee Ref. 2.

^cSee Ref. 1.

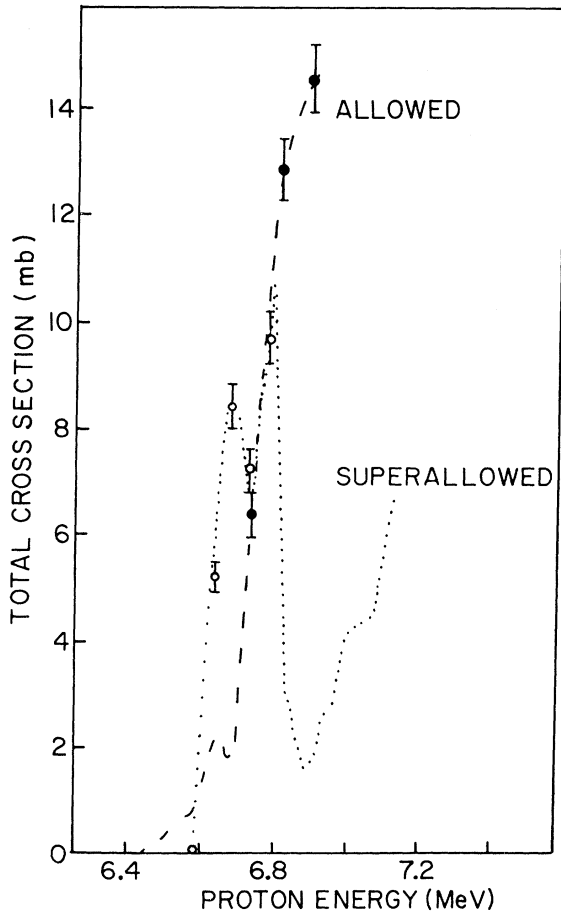


FIG. 5. Comparison of the total cross section versus proton energy for $^{34}\text{S}(p, n)^{34}\text{Cl}$ and $^{34}\text{S}(p, n)^{34}\text{Cl}^m$ (labeled superallowed and allowed, respectively). Error bars indicate the total error expected from all sources.

inent resonances are found to occur in both the (α, n) and (p, n) superallowed excitation curves shown in Figs. 1 to 4. The values for the compound-nucleus excitation energies corresponding to these resonances, 12.9 and 13.9 MeV, are the same within 10 keV for both excitation curves. Hence, it is likely that both reactions are forming the same compound-nucleus states. The full width at half maximum of the 12.9- and 13.9-MeV resonances in the (p, n) excitation curve was found to be 85 and 80 keV, respectively. In the (α, n) excitation curve, these resonances are broader and appear to have more structure.

A possible explanation for the strength of these two resonance regions in ^{35}Cl is that they contain analog states of ^{35}S . In order to help assign isospin values for these resonances, $^{31}\text{P}(\alpha, \alpha_0)^{31}\text{P}$ excitation functions were measured over the two resonance regions at 15 angles. Figure 7 shows the excitation functions in the region of the 12.9-MeV resonance. The position of the $^{31}\text{P}(\alpha, n)$ reso-

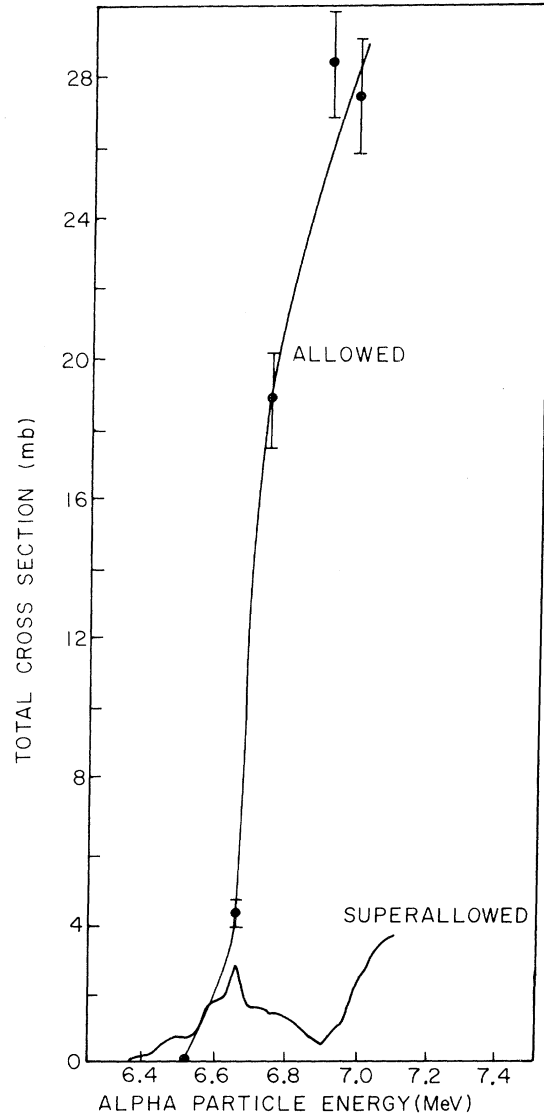


FIG. 6. Comparison of the total cross section versus α -particle energy for $^{31}\text{P}(\alpha, n)^{34}\text{Cl}$ and $^{31}\text{P}(\alpha, n)^{34}\text{Cl}^m$ (labeled superallowed and allowed, respectively). Error bars indicate the total error expected from all sources.

nance is indicated on the figure. As can be seen from the data, no prominent resonance exists in this region, although multiple smaller resonances are evident. In the region of the 13.9-MeV resonance (not shown), the structure of the (α, α_0) excitation function is similar to that seen in Fig. 7. Again, no large resonance is seen.

The lack of any prominent resonance in the (α, α_0) data compared with the (α, n) work indicates a $T = \frac{3}{2}$ rather than $T = \frac{1}{2}$ assignment for the two resonances. For a $T = \frac{3}{2}$ compound state, the (α, α_0) scattering is doubly isospin forbidden (in both entrance and exit channels) compared with singly forbidden (entrance channel only) for the

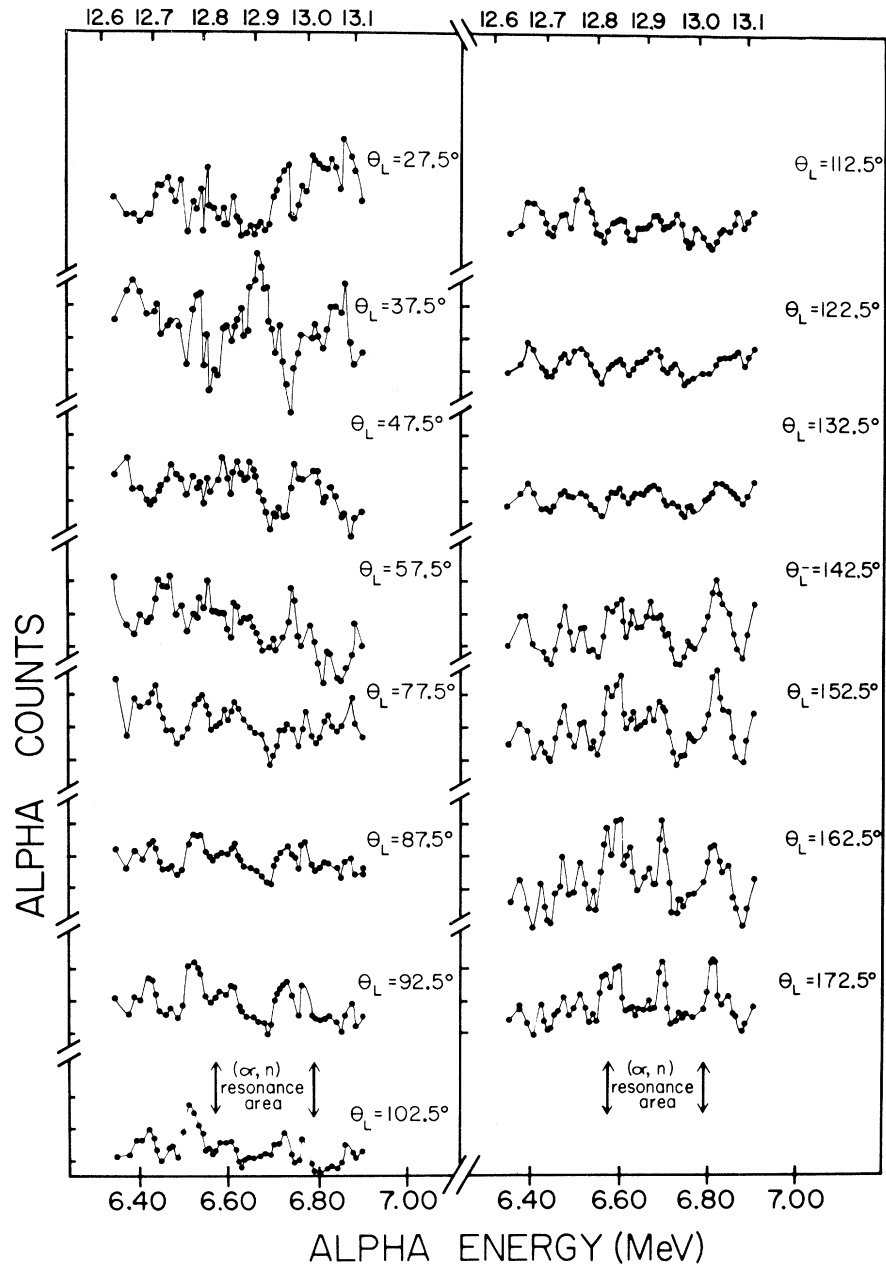
EXCITATION ENERGY IN ^{35}Cl (MeV)

FIG. 7. Excitation curves for $^{31}\text{P}(\alpha, \alpha_0)$ for angles ranging from 27 to 172° with respect to the incident beam.

(α, n) reaction. A small isospin impurity would allow formation of the $T = \frac{3}{2}$ compound state in the (α, n) reaction and would not allow any comparable strength for formation in the (α, α_0) reaction. The large strength seen in both the (p, n) and (α, n) reactions rules out a $T \geq \frac{3}{2}$ assignment for these two levels, since the formation of a $T = \frac{3}{2}$ state is doubly isospin forbidden in the (p, n) reaction and even more highly forbidden in the (α, n) reaction.

IV. SUMMARY

Excitation functions for the reactions $^{34}\text{S}(p, n)^{34}\text{Cl}$ and $^{31}\text{P}(\alpha, n)^{34}\text{Cl}$ have been measured from thresholds at 6438 ± 10 and 6360 ± 10 keV, respectively, to 1.6 MeV above threshold. Two prominent resonance regions were found in both reactions at energies which correspond to excitations of 12.9 and 13.9 MeV in the ^{35}Cl compound nucleus. Since no

corresponding structure was observed in the ^{31}P - (α, α_0) excitation curve, a $T = \frac{3}{2}$ assignment is favored for these levels. The parent states of these resonant levels in ^{35}Cl would occur at 7.4 and 8.4

MeV in ^{35}S . Since the level scheme of ^{35}S above 5-MeV excitation is not yet known, no comparison can be made at this time.

ACKNOWLEDGMENTS

The authors wish to thank the members of their research group for assistance in taking data, in particular A. Aldridge, S. Chen, C. McKenna, R. Sankey, C. Delaune, and M. Kirby. The authors

also thank Dr. S. Edwards and Dr. D. Robson for many helpful discussions and suggestions during the course of this work.

†Research sponsored in part by the Air Force Office of Scientific Research, Office of Aerospace Research under AFOSR Grant No. AF-AFOSR-69-1674, and the National Science Foundation under Grant No. NSF-GP-367.

*Present address: Department of Physics, The University of Kansas, Lawrence, Kansas 66045.

¹A. R. Quinton and W. T. Doyle, Phys. Rev. 101, 669 (1956).

²J. M. Freeman, J. H. Montague, G. Murray, R. E. White, and W. E. Burcham, Nucl. Phys. 65, 113 (1965).

³J. W. Nelson, H. S. Plendl, and R. H. Davis, Phys. Rev. 125, 2005 (1962).

⁴M. K. Mehta, W. E. Hunt, H. S. Plendl, and R. H. Davis, Nucl. Phys. 48, 90 (1963).

⁵B. E. Bonner, G. Richards, D. L. Bernard, and G. C. Phillips, Nucl. Phys. 86, 187 (1966).

⁶D. Birch and J. W. Nelson, Nucl. Instr. Methods 35, 293 (1965).

⁷P. M. Endt and C. van der Leun, Nucl. Phys. A105, 1 (1967).

$^{88}\text{Sr}(d, p)^{89}\text{Sr}$ Reaction in the Region of the $^{88}\text{Sr}(d, n)^{89}\text{Y}^A$ Threshold*

S. A. A. Zaidi, W. R. Coker, and D. G. Martin†

Center for Nuclear Studies, University of Texas, Austin, Texas 78712

(Received 14 May 1970)

$^{88}\text{Sr}(d, p)^{89}\text{Sr}$ excitation curves were measured at 90, 140, 160, and 170° for four states in ^{89}Sr : the $d_{5/2}$ ground state, 1.03-MeV $s_{1/2}$ state, 2.00-MeV d doublet, and 2.45-MeV $d_{3/2}$ state, at deuteron energies from 5.0 to 10.5 MeV. The excitation curves for ground state and 1.03-MeV $s_{1/2}$ state display cusps at the threshold of the charge-exchange-coupled channel, $^{88}\text{Sr}(d, n)^{89}\text{Y}^A$. The data are fit with coupled-channel Born-approximation calculations.

I. INTRODUCTION

The suggestion that charge exchange could couple analogous (d, p) and (d, n) channels was first given by Moore *et al.*,¹ who reported the experimental observation of an anomalous dip in the $^{90}\text{Zr}(d, p)^{91}\text{Zr}(d_{5/2} \text{ ground-state})$ excitation function at 170°, centered on the experimental $^{90}\text{Zr}(d, n)^{91}\text{Nb}^A$ - $(d_{5/2} \text{ analog resonance})$ threshold. A large number of subsequent experiments have provided examples of similar, usually somewhat weaker, anomalies in backward angle ($>130^\circ$) (d, p) or (p, d) excitation functions, for targets $^{91, 92, 94, 96}\text{Zr}$,²⁻⁴ $^{92, 94}\text{Mo}$,³ ^{89}Y ,⁵ ^{80}Se ,⁶ and also ^{40}Ar ,⁷ ^{48}Ca ,⁸ and ^{53}Cr .⁹ In each case an apparent dip in the cross section, roughly an MeV broad, appears centered on the appropriate

charge-exchange (d, n) threshold, providing a beautiful example of the long-predicted but rarely seen threshold cusp phenomenon. Various efforts to find similar effects using lighter- and heavier-mass nuclei have not succeeded.¹⁰

The most dramatic known example of the threshold effect is provided by $^{88}\text{Sr}(d, p)^{89}\text{Sr}(d_{5/2} \text{ g.s.})$ in the vicinity of the lab deuteron energy 7.4 MeV. The cusp, as the data presented here show in comparison with $^{90}\text{Zr}(d, p)^{91}\text{Zr}(d_{5/2} \text{ g.s.})$ data¹¹ at the same angles, is the same width and deeper by nearly a factor of 2. Thus, it provides a harsh test for theoretical descriptions of the threshold effect.

A theory of the (d, p) threshold effect was originally given in terms of the Lane model by Zaidi